Reinvestigation by Phosphorus NMR of Lipid Distribution in Bicelles

Mohamed N. Triba, Dror E. Warschawski, and Philippe F. Devaux
Unité Mixte de Recherche No. 7099, Centre National de la Recherche Scientifique, Institut de Biologie Physico-Chimique, Paris, France

ABSTRACT   Mixtures of dimyristoyl-phosphatidylcholine (DMPC) and dihexanoyl-phosphatidylcholine (DHPC) in water form disks also called bicelles and different bilayer organizations when the mol ratio of the two lipids and the temperature are varied. The spontaneous alignment in a magnetic field of these bilayers above the transition temperature T_m of DMPC is an attractive property that was successfully used to investigate protein structure by NMR. In this article, we have attempted to give an overview of all structural transformations of DMPC/DHPC mixtures that can be inferred from broad band ^{31}P-NMR spectroscopy between 5 and 60°C. We show that above a critical temperature, T_v, perforated vesicles progressively replace alignable structures. The holes in these vesicles disappear above a new temperature threshold, T_h. The driving force for these temperature-dependent transformations that has been overlooked in previous studies is the increase of DHPC miscibility in the bilayer domain above T_m. Accordingly, we propose a new model (the "mixed bicelle" model) that emphasizes the consequence of the mixing. This investigation shows that the various structures of DMPC in the presence of increasing mol ratios of the short-chain DHPC is reminiscent of the observation put forward by several laboratories investigating solubilization and reconstitution of biological membranes.

INTRODUCTION

Since the early 1980s, the group of M. Roberts has been investigating by NMR and other techniques the structure formed by aqueous suspensions of lipids composed by a mixture of two types of phosphatidylcholine (PC): one with two long alkyl chains (dimyristoyl-PC (DMPC) or dipalmi-toyl-PC (DPPC)) and one with two short alkyl chains (dihexanoyl-PC (DHPC) or diheptanoyl-PC) (Gabriel and Roberts, 1984, 1986, 1987; Gabriel et al., 1987; Eum et al., 1989; Bian and Roberts, 1990; Lin et al., 1991). They initially proposed the spontaneous formation of small unilamellar vesicles at low temperatures, when the long-chain lipid is in the gel state (Gabriel and Roberts, 1984, 1986). Later they suggested, for a molar ratio $q = 4$ between the long-chain lipid and the short-chain lipid, the formation of either nonspherical vesicles or bilayer disks (Bian and Roberts, 1990). More recent results by neutron scattering at low-angle, quasielastic light scattering, and electron microscopy confirmed the existence of flat disks as a possible organization of particular lipid mixtures rather than closed vesicles. (Lin et al., 1991; Glover et al., 2001b; Luchette et al., 2001; Nieh et al., 2001, 2002, 2004; Van Dam et al., 2004). The edges of the disks would contain the short-chain lipids whereas the DMPC (or DPPC) would form the central part of the disks.

For temperatures above T_m, the phase transition temperature of DMPC from gel to fluid, the existence of disks was also inferred from ^{2}H and ^{31}P-NMR investigation (Sanders and Schwonek, 1992; Vold and Prosser, 1996; Arnold et al.,

2002). The main interest in the disks, referred to as "bicelles", lays in their propensity to orient themselves in a magnetic field above T_m. This feature provides a mean to orient membrane proteins that can be inserted into (Sanders and Landis, 1995; Howard and Opella, 1996; Prosser et al., 1999) or interact superficially with a phospholipid bilayer (Sanders and Landis, 1994; Vold et al., 1997; Glover et al., 2001a; Lindberg et al., 2003). Bicelles are also used in NMR to provide an anisotropic environment to nonspherical soluble macromolecules. The partial alignment causes residual dipolar coupling that is used to help protein or nucleic acid structure determination (Tjandra and Bax, 1997).

Although the disk structure is well accepted at low temperature and the word bicelle used to designate a lipid disk, several groups believe that an alternative structure could account for the experimental observations of alignment at high temperature. For example, the structure would be composed of multilamellar sheets oriented by the magnetic field containing holes formed by short-chain phospholipids (Gaemers and Bax, 2001; Nieh et al., 2001, 2002; Rowe and Neal, 2003; Soong and Macdonald, 2004; Van Dam et al., 2004). Note that the latter structure is topologically equivalent to the former one (disks of DMPC surrounded by DHPC) and that one cannot prove or disprove either model in a straightforward manner by analysis of a single NMR spectrum. More recently, new types of structures have been proposed for the magnetically alignable phase, namely wormlike micelles or ribbons (Nieh et al., 2004). Despite all the topologies proposed for the alignable structure, we think that only a detailed analysis of NMR data covering low and high temperatures as well as various lipid compositions allows one to apprehend the organization of such lipid suspensions.

Broad band ^{31}P-NMR spectra of mixtures of long-chain PC and short-chain PC have been presented and analyzed already by different groups (Sanders and Schwonek, 1992; Ottiger and Bax, 1998; Picard et al., 1999; Raffard et al., 2000; Arnold et al., 2002). At low temperature, below T_m, what appears as narrow lines can be assigned to small disks in rapid rotation, as we will see later. Above T_m, the existence of two well-differentiated resonances is generally taken as an indication of the spontaneous alignment of lipid disks or sheets in the magnetic field. With a mixture of DMPC and DHPC, the high-field resonance would correspond to DMPC in oriented bilayers and the low-field resonance to DHPC forming disks or hole edges. ^{2}H-NMR with deuterated lipids as well as ^{15}N experiments with uniformly labeled peptides integrated into these structures confirmed their alignment in a magnetic field for $T > T_m$.

A classical hypothesis that we wish to challenge in this article is that of a strict segregation between the two lipids. It forms the basis of the so-called "ideal bicelle model" (Vold and Prosser, 1996). In the temperature range where bicelles orient in the magnetic field, this model cannot explain three main ^{31}P NMR observations: 1), when raising the temperature, the high-field resonance shifts toward higher fields, i.e., toward −15 ppm; 2), when raising the temperature, the low-field resonance shifts even faster to high fields; 3), above another critical temperature, T_v, NMR indicates that a structural modification of the lipid aggregates takes place. In this investigation we show that broad band ^{31}P-NMR, within the framework of the nonsegregated model, allows one to describe the structure of the aqueous suspension of DMPC and DHPC in a wide range of temperature and for different mol ratios $q = [DMPC]/[DHPC]$. We have examined samples with a molar ratio q varying from 2 to 15 and a temperature varying from 5 to 60°C. The nonsegregated model has allowed us to overcome some difficulties of interpretation that were associated with previous NMR investigation limited to small q values and/or to temperatures below 40°C.

MATERIALS AND METHODS

Sample preparation and manipulation

1,2-dimyristoyl-*sn*-glycero-3-phosphocholine (DMPC) and 1,2-dihexanoyl-*sn*-glycero-3-phosphocholine (DHPC) were purchased from AVANTI polar lipids (Alabaster, AL). Most samples were prepared in 500 μL of water at a total lipid concentration c_L of 25% (w/w). The lipid suspensions were submitted to agitation at temperatures below and above T_m (≈ 23°C). For small values of the molar ratio $q = [DMPC]/[DHPC]$, it was necessary to lower the temperature below T_m to obtain a fluid sample that could be easily homogenized. When the temperature was raised above T_m, the sample became progressively viscous but remained transparent. For temperatures above a critical value T_v (function of q but typically above 40–45°C) the sample became milky and less viscous. For $q > 9$ the sample was milky at all temperatures and a macroscopic phase separation took place below T_m with a fluid and transparent supernatant on the top of a milky phase. Homogenization had to be done above T_m in such cases. The transfer to NMR

tubes was done at the temperature for which the samples were the more fluid and homogeneous.

NMR experiments

All experiments were carried out on a Bruker AVANCE DMX 400-WB spectrometer (Wissembourg, France) with a 9.7 Tesla field. The corresponding frequency for ^{31}P nuclei is 162 MHz. The insert that contains the sample is inserted in a classical NMR tube with a diameter of 10 mm (New Era Entreprises, Vineland, NJ). This tube contained enough D$_2$O to allow us to lock the spectrometer field during acquisition. It contained also, in some instances, a phosphate buffer the signal of which is used as a frequency reference that we have arbitrarily fixed at 2 ppm. The position of the narrow line associated to isotropically tumbling micelles is then ~ -1 ppm. The variation with temperature of this reference was tested and was found very small. ^{31}P (90°) pulses were obtained in 26 μs. To avoid heating the sample, we used a very low ^{1}H continuous decoupling power (6 kHz). Hahn echo pulses were used with a delay of 40 μs. The delay between each cycle was 5 s.

RESULTS

Transition temperatures

^{31}P-NMR spectra of various mixtures of DMPC and DHPC in water were recorded at different temperatures and molar ratios. Fig. 1 shows the spectra of samples with different mol ratios q of DMPC/DHPC. Spectra were obtained by heating the samples progressively from 16 to 60°C. Small differences in line shapes and intensities were observed when the spectra were obtained by cooling the samples but peak positions and relative intensities were unaffected (data not shown). Figs. 2–4 show NMR spectra of samples with different ratios of DMPC/DHPC recorded, respectively, at low temperature, i.e., below the transition temperature T_m of DMPC (Fig. 2), near T_m (Fig. 3), and at high temperature (Fig. 4). These ^{31}P-NMR spectra of the two lipids in aqueous suspension demonstrate a complex variation with temperature and mol ratios.

To facilitate subsequent spectral analysis we have split the following sections into temperature intervals. We used three specific temperatures T_m, T_v, and T_h, which appear naturally as transition temperatures in the NMR spectra when heating a sample. Each temperature interval will eventually be associated with a particular structure of lipid aggregates in the discussion section. The most obvious one, T_m, is the phase transition temperature of DMPC. $T_m = 23$°C for pure DMPC in water (q infinite). But T_m decreases slightly when the proportion of DHPC increases, as shown before by Roberts and co-workers by adding a short-chain lipid to DPPC (Bian and Roberts, 1990). Thus, for small values of q, an effective T_m should be introduced in principle for each q value. On the ^{31}P-NMR spectra, this transition temperature is determined by the sudden occurrence of a broad signal, as will be shown below.

T_v is a second transition temperature associated with the appearance of a signal at −15 ppm. This temperature also depends upon q. At T_v the number of distinguishable
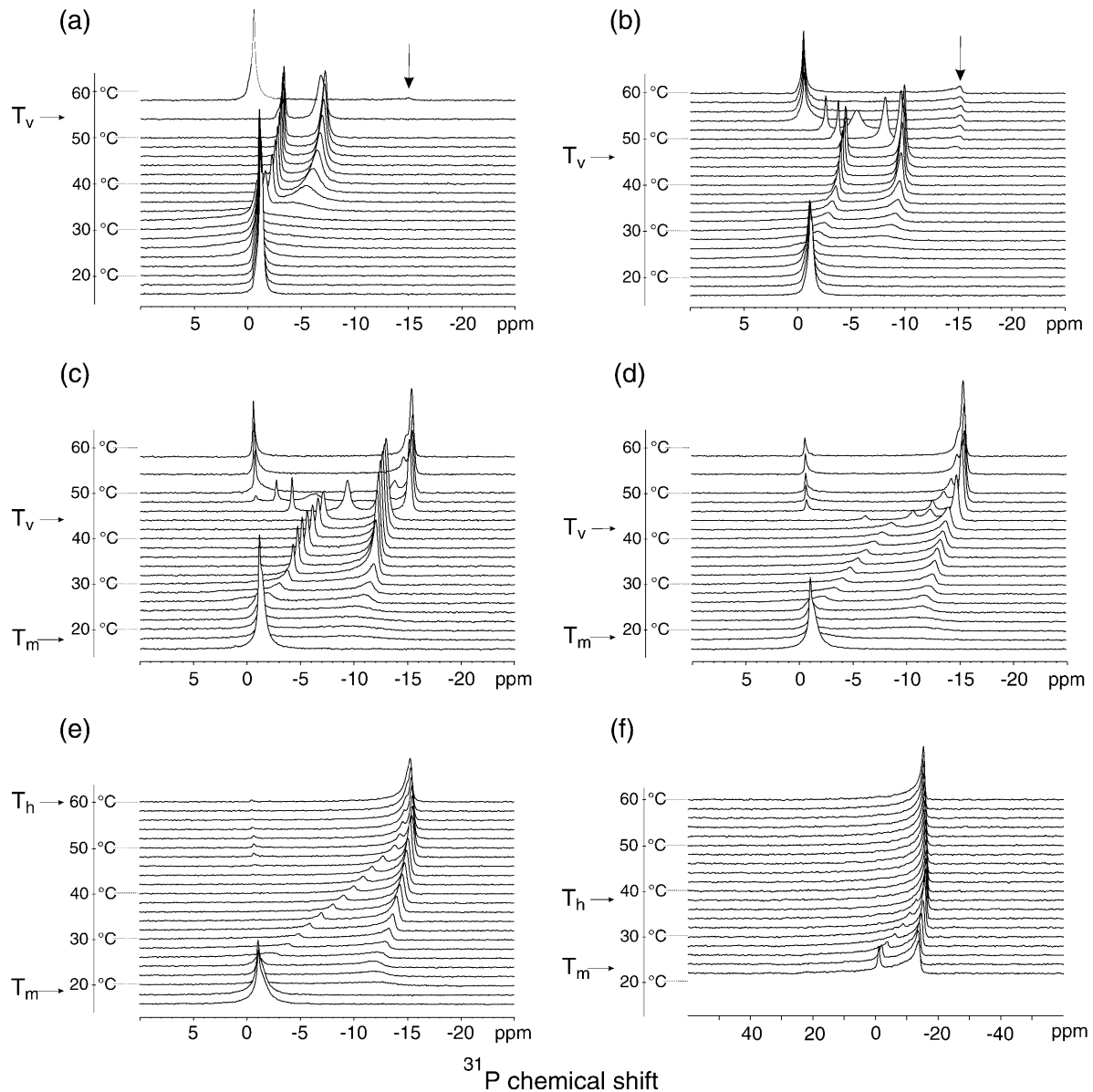
FIGURE 1 ^{31}P-NMR spectra at 162 MHz of different DMPC/DHPC mixtures at temperatures between 16 and 60°C. Spectra were recorded from low to high temperature; q values were, respectively: (a) 2.5; (b) 3; (c) 4; (d) 5; (e) 6; (f) 10. In all samples the percentage of lipid/water was 25% (in weight). Vertical arrows indicate the small resonances at −15 ppm. Note that the chemical shift scale is different for $q = 10$. For each spectrum 128 acquisitions were collected. A line broadening of 10 Hz (50 Hz for $q = 10$) was applied before Fourier transformation. The delay between acquisitions at different temperatures was 20 min.

resonance peaks suddenly increases. See the discontinuities in the evolution of NMR spectra around 45°C in Fig. 1 and the spectrum corresponding to $q = 4$ in Fig. 4. T_v is above 50°C for $q = 2.5$, around 48°C for $q = 3$, and around 42°C for $q = 5$. For $q \geq 6$, T_v is very close or merged with T_m and cannot be determined because no important discontinuity in the evolution of the NMR spectrum is observed.

A third characteristic temperature, T_h, can be associated with the merging of the two high-field peaks near −15 ppm. $T_h = 38°C$ for $q = 10$ and $T_h = 60°C$ for $q = 6$ (Fig. 1). For $q \leq 5$, T_h is above 60°C and was not determined in this investigation.

We will now analyze in more details the NMR spectra within the different temperature ranges.

^{31}P-NMR spectra at low temperatures ($T < T_m$)

For low temperatures ($T < T_m$), the ^{31}P-NMR spectrum of a mixture of DHPC and DMPC is often described as a single narrow resonance. Fig. 2 a shows a series of ^{31}P-NMR spectra recorded at 16°C with q included between 2 and 8. For low q values, the spectrum is a narrow but asymmetrical doublet formed by the superposition of two Lorentzian lines near −1 ppm, which is the resonance frequency of an
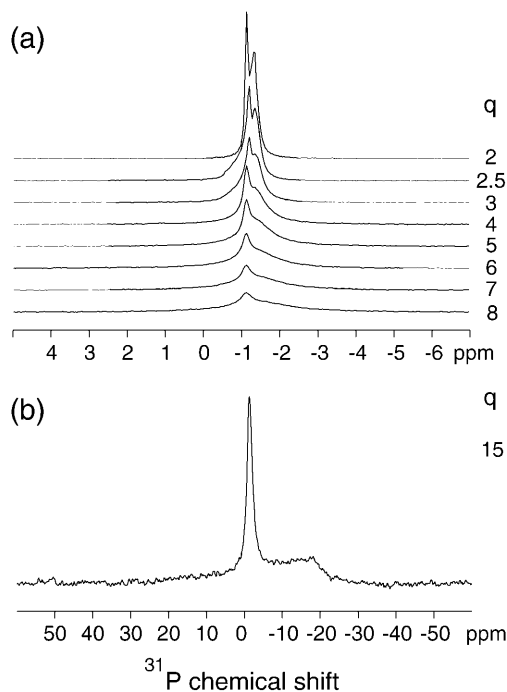
FIGURE 2 ^{31}P-NMR spectra at 16°C of DMPC/DHPC mixtures with different q values: (a) q between 2 and 8; (b) $q = 15$. Note that the chemical shift scale is different for $q = 15$. A line broadening of 10 Hz (50 Hz for $q = 15$) was applied before Fourier transformation.

isotropic sample undergoing rapid motion (see Materials and Methods). Samples are transparent and fluid. A deconvolution of the spectrum recorded for $q = 2$ and $T = 16°C$ indicated linewidths of 170 and 390 Hz for the low- and high-field resonances, respectively, with a difference in chemical shift of 30 Hz (Triba, 2003). These linewidths increase with q but the ratio between the integrals of both resonances remains close to q, indicating that the low-field one probably corresponds to DHPC and the high-field one corresponds to DMPC. At some point, both lines overlap (Fig. 2 a). For $q = 10$ (Fig. 2 b), the ^{31}P-NMR spectrum contains a narrow ^{31}P resonance near -1 ppm, which is superimposed to a broad ''bilayer'' component with $\Delta\sigma >$ 50 ppm, characteristic of a bilayer in the gel phase ($L_{\beta'}$). The maximum intensity at high field is ~ -15 ppm but the low-field limit is practically impossible to determine. At this point, samples stayed fluid but became milky.

Fig. 3 shows a series of spectra recorded with increasing q values at 22°C, which is close but in principle below the transition temperature of DMPC. For $q \leq 3$, the spectra contain narrow lines and the corresponding samples are transparent and fluid. For $q \geq 4$ the spectrum differs considerably: it contains a narrow component near -1 ppm superimposed to a broad component and the corresponding samples become viscous and slightly translucent. For $q = 4$, the broad component has a line shape typical of phospholipids in nonoriented vesicles, yet the overall splitting of $\Delta\sigma$
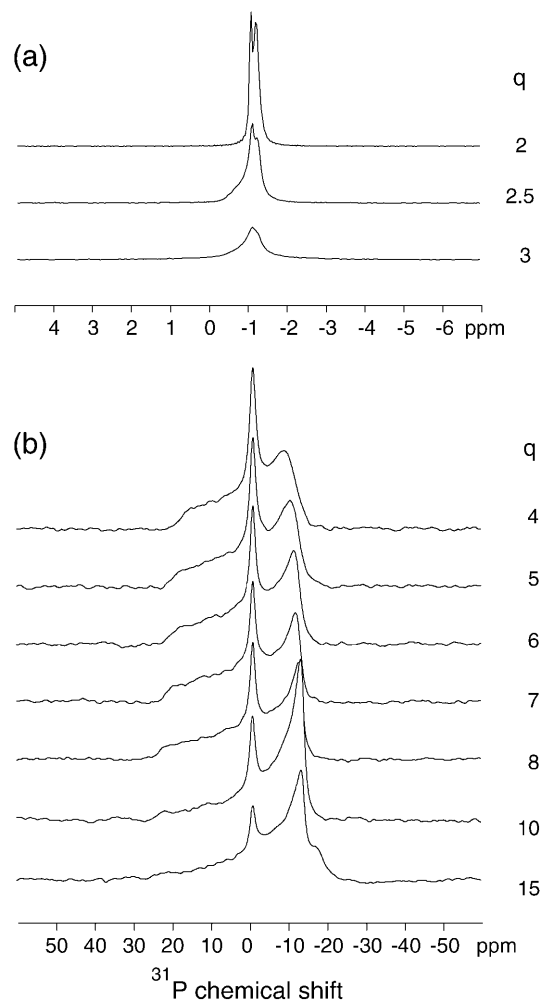
FIGURE 3 ^{31}P-NMR spectra at 22°C of DMPC/DHPC mixtures with different q values: (a) q between 2 and 3; (b) q between 4 and 15. Note that the chemical shift scale is different in panel b. A line broadening of 10 and 50 Hz, respectively, was applied for panel a and panel b before Fourier transformation.

~ 30 ppm is below the usual splitting characteristic of lipid vesicles in the fluid phase L_α. Despite the variety of line shapes observed, integrating the signals is still consistent with our assignment of the isotropic one to DHPC and the broad one to DMPC. Note that the same spectrum appears in Fig. 1 c but at a scale that does not enable one to see the broad component at 22°C, with a peak near -10 ppm. Although the interpretation is not trivial, there is undoubtedly a change in the lipid organization between 16 and 22°C when $q \geq 4$, i.e., slightly below the transition temperature of pure DMPC from gel to fluid phase.

^{31}P-NMR spectra at high temperature ($T > T_m$)

For temperatures above T_m, mixtures of DMPC and DHPC give rise to more complicated ^{31}P-NMR spectra. It becomes necessary to discriminate $q < 6$ and $q \geq 6$.
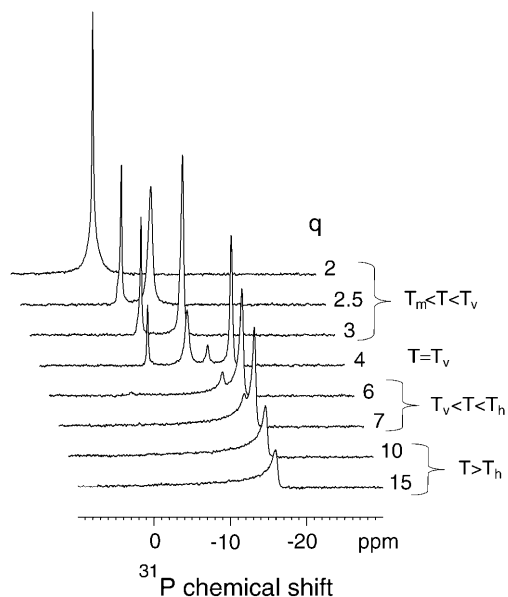
FIGURE 4 ^{31}P-NMR spectra at 46°C of DMPC/DHPC mixtures with different q values between 2 and 15. A line broadening of 10 Hz was applied before Fourier transformation.

Mol ratio q = [DMPC]/[DHPC] < 6

When samples are heated above T_m, the broad component narrows down, grows in intensity, and shifts toward high fields (Fig. 1). Eventually the ^{31}P-NMR spectrum is composed of two well-separated narrow lines. This narrowing of the broad phosphorus component has been assigned already in the literature to the spontaneous alignment of bicelles or of perforated lamellar sheets in the magnetic field (Sanders and Schwonek, 1992; Nieh et al., 2001). The low-field peak would correspond to DHPC in the edges of bicelles or holes and the high-field peak would correspond to DMPC in the bilayer. At this point, the samples are still transparent but become very viscous. The difference in chemical shift between the two resonances varies from 4 to ~10 ppm, depending upon q and temperature (Fig. 1). The two narrow peaks move up field when the temperature increases but at a different rate, thus their mutual splitting decreases.

Just below T_v, the signal that is classically assigned to DMPC reaches its up-field limit, which is around −7 ppm for q = 2.5, around −10 ppm for q = 3, around −12 ppm for q = 4, and around −14 ppm for q = 5. T_v is a new transition above which all samples give spectra with a peak at −15 ppm. The presence of this new peak reveals the appearance of a new structure, which has a slow motion on the ^{31}P-NMR timescale.

Above T_v, depending on the temperature, spectra contain three or four peaks. In Fig. 4, for example, the spectrum corresponding to q = 4 and T = 46°C contains four narrow resonances between −4 and −15 ppm. The same spectrum is present also in Fig. 1 c where it appears as a transition spectrum between two temperature domains. The same resonance at −15 ppm appears in all Fig. 1 spectra (for Fig.

1, a and b, see vertical arrows). At this point, samples become fluid and milky. After a few minutes, a phase separation occurs with a transparent supernatant above this milky phase.

Mol ratio q = [DMPC]/[DHPC] ≥ 6

For q ≥ 6, T_v is close to T_m. When the temperature is between $T_m \approx T_v$ and T_h, the spectra are composed of two asymmetric signals, which become closer to each other as the temperature is raised (Fig. 1 f). Integration of those signals allowed us to assign the high field signal to DMPC and the low field signal to DHPC. Eventually, at T_h, both signals merge. At this temperature, samples are fluid and milky, and appear to be homogenous.

DISCUSSION

As already apparent in the Results section, the structure of bicelles is very dependent on the temperature and on the mol ratio q of long-chain PC over short-chain PC. We defined, in the above sections, three characteristic temperatures, T_m, T_v, and T_h on the basis of spectral evolution when going from low to high temperature. The objective of this Discussion is to shift from the NMR results to a molecular interpretation as thorough as possible that should eventually lead to results that are technique independent. Clearly it will be necessary to divide the discussion in sections associated with various temperature domains. When indispensable we will have to subdivide also into domains on the basis of q values.

Low temperatures (T ≤ T_m)

T_m is the most obvious characteristic temperature and corresponds to the transition of pure DMPC. We have assumed, like most researchers in this field, that below T_m and for low to intermediate q values (q < 9), bicelles are flat disks with an almost perfect segregation between DMPC forming bilayers, and DHPC being clustered on the edges of the disks (Bian and Roberts, 1990; Lin et al., 1991; Glover et al., 2001b; Luchette et al., 2001; Nieh et al., 2001, 2002, 2004; Van Dam et al., 2004). This is also true for 0.5 < q < 2 whatever the temperature, however, we have not explored the latter domain (Glover et al., 2001b; Luchette et al., 2001). The narrow resonances near −1 ppm indicate a rapid Brownian motion of the disks, the anisotropy of the phosphate chemical shift being averaged out by the rapid motion of the bicelles. Thus, bicelles are not oriented at low temperatures. The diamagnetism of the lipid chains of a single disk is insufficient to generate a momentum big enough to overcome thermal randomization in a magnetic field of 9 Tesla (Hare et al., 1995). A rapid motion implies small disks. Besides ^{31}P- and ^{2}H-NMR data, another simple argument in favor of small particles is the macroscopic fluidity and the transparence of the samples below T_m.

Why do we see a doublet near −1 ppm rather a single peak? Two phosphatidylcholine molecules like DMPC and DHPC, undergoing rapid isotropic motion, should have the same phosphorus chemical shift. We have verified that the two lipids in organic solvents are indeed indistinguishable by high-resolution NMR. Furthermore, in water, the ratio between the integrals of both resonances corresponds to the molar ratio q. This strongly suggests that the low-field peak corresponds to DHPC and the high-field peak to DMPC as previously suggested. The difference in chemical shifts, which is seen in Fig. 2 a, between DHPC and DMPC is likely to be caused by different environments. The lamellar phase of DMPC bilayers differ from the highly curved DHPC edges where water is more accessible. Furthermore, DHPC is more soluble in water than DMPC and exchanges rapidly with the aqueous environment (Glover et al., 2001b). Thus, the average local polarity of DMPC and DHPC can be slightly different in bicelles. The linewidth increase with q of both ^{31}P lipid resonances can be explained by an increase of disk radii because, for q values between 2 and 6, the radius of a segregated disk would be between 10 and 40 nm (Vold and Prosser, 1996).

When the temperature becomes close to T_m, and $q > 3$, there is an important change in the shape of NMR spectra. Indeed, between 16 (Fig. 1) and 22°C (Fig. 2) a broad component appears for those samples and reveals a transition to a different physical state. The apparent paradox is that this transition corresponds to less motion at 22 than at 16°C. Thus, the lipid aggregates tumble suddenly at a slower rate, precisely when bilayers are more fluid.

One possibility is that disks suddenly fuse at T_m, which would increase their size, hence their rotational correlation time. Another likely interpretation is that the melting of DMPC from L_β to L_α phase renders disks susceptible to interact with each other via van der Waals interactions or long-range forces and permits the formation of stacks, chains, or lattices of disks (Bolze et al., 2000; Spalla, 2000; van der Kooij et al., 2000; Duneau et al., 2003; Leng et al., 2003). A lattice of interacting disks could resemble a highly perforated lamella of lipids and the small differences would not be detected by NMR. One reason for favoring the onset of a cooperative effect is that the anisotropy of the magnetic susceptibility is insufficient to orient a single disk in the magnetic field whereas a lattice or a pile of disks could stabilize their alignment above T_m (Hare et al., 1995).

In any case, we believe the sample at $T \approx T_m$ is composed of misaligned interacting disks, with DHPC in the edges, almost perfectly segregated from DMPC in the disk planes. This is consistent with the respective area of ^{31}P-NMR signals where the broad line would correspond to DMPC and the narrow line to DHPC (see Fig. 3 b, for example). Although bicelles are large and unoriented, as shown by the broad DMPC line, the edge signal (DHPC) is perfectly isotropic.

For $q \geq 9$, the observation of transparent samples does not hold true below T_m, indicating the presence of larger objects.

Centrifugation of such mixtures indicated the presence of disks (in the transparent supernatant) coexisting with vesicles in the gel phase in the milky phase (Bian and Roberts, 1990). The presence of vesicles in the gel phase is confirmed by the appearance of a broad component ($\Delta\sigma > 50$ ppm) as shown by Fig. 2 b that corresponds to $q = 15$. Of course, for q infinite (pure DMPC) the sample contains only vesicles.

Intermediate temperatures $T_m < T < T_v$

Increased DHPC miscibility in the bilayer domain at high temperature

In previous works on bicelle systems, some authors have tried to explain the structural changes observed with temperature by an increase of the amount of free DHPC in water. As proposed by Ottiger et al. (Ottiger and Bax, 1998) and more recently by van Dam et al. (2004), this increase of the number of DHPC molecules in water when the sample is heated should explain, for example, the increase of the bicelle size for diluted systems ($c_L = 3\%$ (w/w)). Nevertheless, for the concentrated system that we studied here ($c_L = 25\%$ (w/w)), the concentration of free DHPC that was estimated to be ~5 mM (Ottiger and Bax, 1998; Struppe and Vold, 1998; Ramirez et al., 2000; Glover et al., 2001b; Van Dam et al., 2004) represent <5% of the total amount of DHPC when $q = 3$. Moreover, van Dam et al. (2004) have measured that the concentration of this free DHPC increases by only 2 mM from 25 to 50°C. For $q = 3$ and a lipid concentration of 25% (w/w), this increase corresponds to a variation of only 2% of molar ratio of DMPC/DHPC inside the aggregates formed by the two lipids. Consequently, for the concentration that we studied, the temperature variation of the concentration of free DHPC cannot explain the changes of structures observed when the sample is heated.

On the contrary we propose that, for a concentrated sample, the effect of free DHPC in water can be neglected. Thus, the mixture of the two lipids can be seen at first approximation as a pseudobinary mixture (Cevc and Marsh, 1987). These kinds of lipid mixtures have been widely studied, particularly when the two lipids differ only by the length of their hydrophobic chains (Lee, 1977; van Dijck et al., 1977; Feigenson and Buboltz, 2001). All these studies showed that even if a segregation can be observed between the two lipids, this segregation is never total. This is true in particular when the temperature is above the main transition temperatures of both lipids. Thus, we believe that the DHPC rich domain, which forms the edges of bicelles or holes, contains a small amount of DMPC and that the DMPC rich domain, which forms the bilayer, should also contain a small amount of DHPC. Moreover, Gibbs law is also fulfilled in this pseudobinary system, which implies that as long as edges and bilayers coexist in the sample, the composition of each domain depends on temperature but not on q.

We call ε the fraction of DHPC molecules inside the DMPC-rich section and ε' the fraction of DMPC molecules inside the DHPC-rich section:

$$\varepsilon = \frac{n_{\text{DHPC}}^{\text{bilayer}}}{n_{\text{DMPC}}^{\text{bilayer}} + n_{\text{DHPC}}^{\text{bilayer}}} \quad \text{and} \quad \varepsilon' = \frac{n_{\text{DMPC}}^{\text{edge}}}{n_{\text{DMPC}}^{\text{edge}} + n_{\text{DHPC}}^{\text{edge}}},$$

where $n_{\text{DMPC}}^{\text{bilayer}}$ and $n_{\text{DMPC}}^{\text{edge}}$ are the number of DMPC molecules, respectively, in the bilayer and in the edge, and $n_{\text{DHPC}}^{\text{bilayer}}$ and $n_{\text{DHPC}}^{\text{edge}}$ the number of DHPC molecules, respectively, in the bilayer and in the edge.

Several laboratories have already suggested models above T_{m} implying a partitioning of the two phospholipids (Eum et al., 1989; Bian and Roberts, 1990; Sanders and Schwonek, 1992; Van Dam et al., 2004). Sternin et al. (2001) attempted to measure cross-relaxation between DMPC and DHPC at 35°C but no crosspeak was detected. This result demonstrates that, for this temperature domain, ε and ε' are below 0.1, the detection limit of the method.

Due to the difference in chain lengths of the two lipids, ε and ε' are likely to be small. Nevertheless, ε' is probably nonzero because DHPC is fluid at all temperatures in this study. On the other hand, ε is probably close to zero below T_{m} and nonzero above T_{m}. The small value of ε' means that for $q > 2$, $n_{\text{DMPC}}^{\text{edge}}$ can be neglected: $n_{\text{DMPC}}^{\text{bilayer}} \approx n_{\text{DMPC}}$, where n_{DMPC} is the total number of DMPC molecules in the sample. On the other hand, ε can be deduced from NMR experiments. Following Sanders' approach (Sanders and Schwonek, 1992), which is based on the hypothesis of a fast exchange of DHPC between bilayers and edges, we have derived a formula in the Appendix of this article, which links q and ε to the chemical shifts variation of the two resonances assigned, respectively, to DHPC and DMPC. The expression A4 of $\Delta\omega_{\text{DHPC}}/\Delta\omega_{\text{DMPC}} = (\omega_{\text{DHPC}} - \omega_{\text{DHPC}}^{\text{iso}})/(\omega_{\text{DMPC}} - \omega_{\text{DMPC}}^{\text{iso}})$ established in the Appendix takes the form:

$$\frac{\Delta\omega_{\text{DHPC}}}{\Delta\omega_{\text{DMPC}}} = Aq + B, \quad (1)$$

where A and B depend on the temperature only. The left-hand part of this equation is measurable on the ^{31}P-NMR spectra and could also be applied, to some extent, to ^{13}C-NMR or ^{2}H-NMR. Although similar to Sanders' formula, we have used slightly more general assumptions as explained in the Appendix and propose a formula that allows a linear fit of the experimental data.

Experimental values of $\Delta\omega_{\text{DHPC}}$ and $\Delta\omega_{\text{DMPC}}$ were measured only when two signals were present in the spectrum and when integration of those signals allowed an unambiguous assignment, respectively, to DHPC and to DMPC. Plots of experimental values of $\Delta\omega_{\text{DHPC}}/\Delta\omega_{\text{DMPC}}$ as a function of q are shown in Fig. 5 for five different temperatures.

At each temperature, the variation is linear with q, as predicted by the theory. This result validates previous
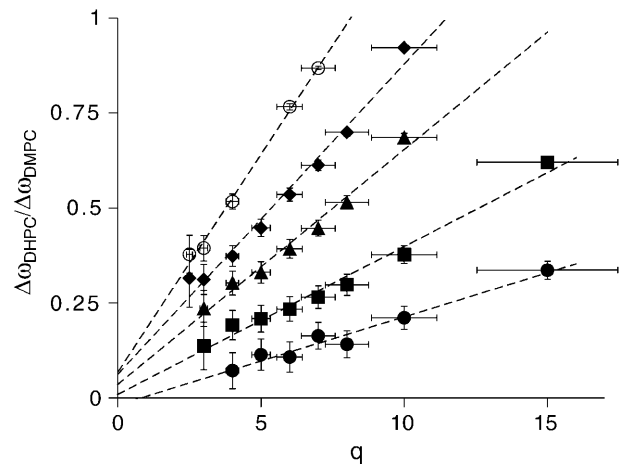

FIGURE 5 Variation of $\Delta\omega_{\text{DHPC}}/\Delta\omega_{\text{DMPC}}$ as a function of q for different temperature values. Experimental points were obtained, respectively, at 26°C (●), 28°C (■), 32°C (▲), 36°C (♦), and 44°C (○). Horizontal error bars correspond to the errors associated with the weighing of the lipids (± 1 mg). Vertical error bars are associated with the uncertainty in the measure of lipid resonance frequencies (± 0.5 ppm). Linear fits were obtained using least-square minimization.

hypotheses on fast exchange of DHPC molecules between edges and bilayers and on the composition of the bilayer that is, at first approximation, only temperature dependent. Because the slope of each line in Fig. 5 is directly related to ε, according to Eq. A4, we were able to determine the variation of ε with temperature (Fig. 6, *open circles*). As expected from previous reports on lipid mixtures (Lee, 1977; van Dijck et al., 1977) we find that ε is close to zero when the temperature is below or close to T_{m}. This result is also consistent with previous reports that showed an important segregation of DMPC and DHPC below T_{m}. Finally, our results are also consistent with the absence of correlation observed by Sternin and co-workers at 35°C (Sternin et al.,
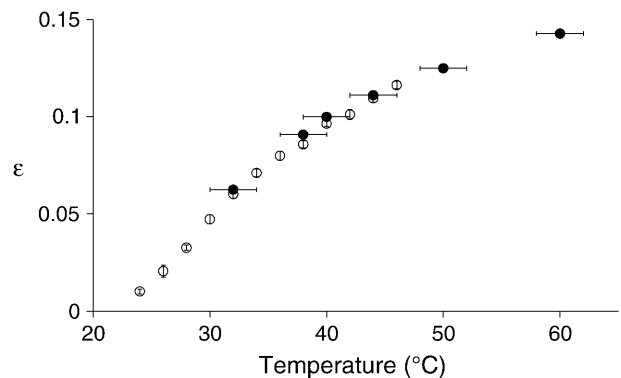

FIGURE 6 Molar fraction ε of lipids with a short chain (DHPC) in the bilayer section as a function of temperature. Open circles are deduced from the slopes of the linear fits in Fig. 5 according to Eq. A4 in the Appendix. Full circles are deduced from the value of q at T_{h} (Eq. 5).

2001) because we find $\varepsilon \approx 0.075$ at this temperature, below the detection limit of ^{1}H NOESY.

One can also infer from Fig. 5 that the straight lines intersect close to the origin. According to Eq. A4, this shows that when DHPC is confined in the edges ($\varepsilon \approx 0$), the signal of this molecule should be close to the isotropic frequency. This is a confirmation of the result obtained close to T_m. As a consequence, above T_m, DHPC exchanges rapidly between edges and bilayers and the DHPC ^{31}P resonance is an average between the edge resonance (isotropic) and the bilayer resonance (that of DMPC). Raising the temperature, hence ε, increases the amount of DHPC molecules in the DMPC bilayer domain. This, and this only, explains why the resonance frequency of DHPC moves away from the isotropic frequency, and closer to that of DMPC, when raising the temperature. This clarifies one of the three observations that none of the classical models, perfectly segregated bicelles or perforated lamellae, could explain.

The mixed bicelle model

No hypothesis was made in the previous paragraphs on the shape of the object formed above T_m. Indeed, the method we used to measure ε is valid for each structure proposed in the literature (disks, perforated lamellae, ribbons...) (Sanders and Schwonek, 1992; Gaemers and Bax, 2001; Nieh et al., 2004). Nevertheless, we will show now that all observations can be explained with the ''disk'' hypothesis and we will show the implication of the variation of ε in the disk model. As opposed to the ''ideal bicelle model'' proposed by Vold and Prosser (1996) where DHPC and DMPC are perfectly segregated even above T_m, the model we propose takes into account the fact that the two lipids are mixed in each domain of the disk. We call this the ''mixed bicelle model''. We now show the implications of the mixed bicelle model on the size of disks.

By analogy with the calculation of Vold and Prosser (1996), we can predict the radius of a mixed bicelle. However we improve the formula generally used to estimate the disk radius. First, the Vold-Prosser formula was obtained by considering the ratio between the surfaces occupied by bilayers and edges. However, the surface occupied by DHPC lipids in edges is not well known (Glover et al., 2001b; Van Dam et al., 2004) and the radius obtained strongly depends on it. Indeed, depending on the authors, this surface is taken equal to the surface of a DMPC headgroup in a bilayer (Vold and Prosser, 1996; Nieh et al., 2001; Arnold et al., 2002) or equal to the surface of a DHPC headgroup in a micelle (Glover et al., 2002; Van Dam et al., 2004). A more appropriate way to estimate the bicelle radius is to use the ratio q_v between the volumes occupied by bilayers and edges. In this case, the bicelle radius depends on the volumes of lipids, which are well known, linearly depend on their hydrophobic chain lengths, and do not depend on the local curvature of the aggregates (Small, 1986).

Another improvement can be made by taking into account the fact that the fully extended hydrophobic chains of DMPC are 9 Å longer than the fully extended hydrophobic chains of DHPC (Tanford, 1991). To consider this mismatch, we assume that bicelle edges have an elliptical profile rather than a circular one. For the thickness of the bilayer ($2r_{//}$) we use the value of 40 Å and for the thickness of the edge ($r_\perp$) we use the value of 11 Å (Fig. 7, a and b). The radius of such a bicelle can then be written (Eq. A8):
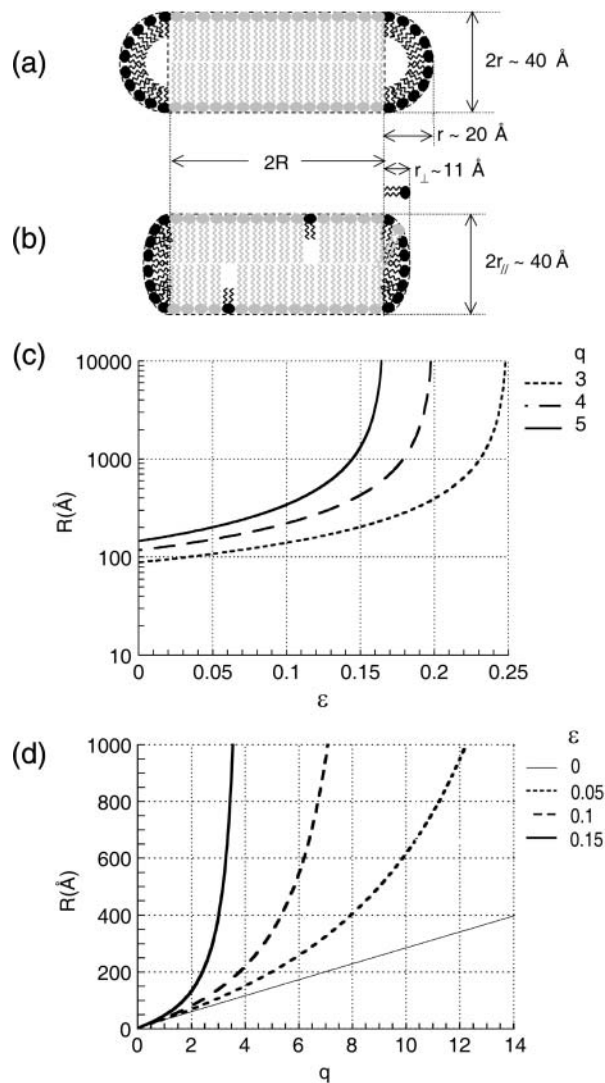

FIGURE 7 Schematic representation of a bicelle with either (a) circular or (b) ellipsoidal edges. Theoretical variation of the bicelle radius R as a function of: (c) the mol fraction ε of DHPC in the bilayer section, for several q values indicated in the figure; (d) the mol ratio q between DMPC and DHPC in the sample, for several ε values indicated in the figure. The thin straight line corresponds to the ''ideal bicelle model'', i.e., to a situation where the short-chain lipids would always be segregated in the bicelle edges. For this simulation, the volumes of DHPC and DMPC molecules, respectively, are 660 Å^3 and 1090 Å^3 (Small, 1986) so that $\lambda = 0.61$, and $r_\perp = 11$ Å (Tanford, 1991). Note that for $\varepsilon > 0$, the formula diverges.

$$R = \frac{1}{4}r_\perp q_v \left(\pi + \sqrt{\pi^2 + \frac{32}{3q_v}} \right). \tag{2}$$

The radius obtained is proportional to $r_\perp$. This indicates that if one uses a circular cross section for the edge, the bicelle radius is strongly overestimated. This theoretical result can explain the mismatch between the radius measured in recent experiments and the radius predicted using the classical formula (Van Dam et al., 2004). For example, using dynamic light scattering, van Dam et al. (2004) have measured the value of $r' = r_\perp + R$ for a diluted sample ($c_L = 5\%$ (w/w)) at 25°C and $q = 1$. They found that $r' = 41.5$ Å, which is much smaller than the 94 Å predicted by the classical formula. To reconcile the classical formula with the experimental results, these authors have proposed to consider that >60% of the DMPC would actually be in the edges. For $q = 1$, this would correspond to $\varepsilon' \approx 0.4$. Using an ellipsoidal cross section for the disk edge one can obtain the correct radius (using Eqs. A8 and A9 with $\lambda = 0.61$ and $\varepsilon = 0$) providing that $\varepsilon' = 0.03$, which implies only 3% of DMPC in the edges, a much more realistic value.

For $q > 2$, the radius formula simplifies into Eq. A11:

$$R \approx \frac{\pi}{2}r_\perp \times \frac{q}{\lambda} \times \left[\frac{1 + \varepsilon(\lambda - 1)}{1 - \varepsilon(q + 1)} \right]. \tag{3}$$

Fig. 7, c and d, show the increase of the theoretical radius R of the bicelles with q and ε. The variation of ε with temperature (Fig. 5) indicates that the bicelles radius should also increase when the sample is heated. The increase of disk radius with temperature was observed recently by dynamic laser light scattering (Van Dam et al., 2004).

Quality of bicelles alignment

Bicelles alignment, for $q > 2$ and $T > T_m$, results from an increase of their magnetic susceptibility anisotropy and their cooperativity (Hare et al., 1995). The distribution of bicelles in a cone around their average position is called the mosaic spread and is estimated by looking at the asymmetry of the ^{31}P resonances. With bicelles, depending on temperature and sample history, narrow quasisymmetrical lines (width at half-height below 1 ppm) can be obtained, corresponding to a mosaic spread of ~6° (Arnold et al., 2002). In addition to their angular distribution, bicelles also oscillate rapidly (on the ^{31}P-NMR timescale) in a cone around their average position. The aperture of this cone has an effect on the ^{31}P chemical shift of the DMPC resonance (see Appendix). Perfect instantaneous alignment, which would result in a high-field resonance at the maximal ^{31}P chemical shift anisotropy value, i.e., −15 ppm, is not observed

Nevertheless, the DMPC ^{31}P resonance shifts toward high fields when the temperature is increased above T_m. This is an indication that bicelles alignment improves with temperature (Ottiger and Bax, 1998). The alignment of bicelles will improve if their radius increases. Increasing the temperature augments ε, hence the bicelle radius as shown by Eq. A11, which in turn improves bicelles alignment and shifts the DMPC ^{31}P resonance to higher fields. In addition, increasing the radius will most likely increase bicelle interactions (Bolze et al., 2000), friction, and inertia against Brownian motion, and contribute to a better alignment. Here again, only the mixed bicelle model can so far satisfactorily explain such a frequency shift with temperature.

When the temperature is increased from ~22 to ~42°C, ε raises from 0 to ~0.1. As an example, for $q = 5$, the high-field resonance shifts from −10 ppm (with a very high mosaic spread; see Fig. 3 b) to −14 ppm (Fig. 1 d). This corresponds to bicelles radius increasing from ~150 Å up to 350 Å and oscillating in a cone which aperture drops from ~21° down to ~14° around their average position. In all cases, the highest chemical shift measured, hence, the best alignment, is obtained just below T_v.

High temperatures ($T \geq T_v$.)

Structural changes

Above T_v, a new transition is observed by NMR and is accompanied by a modification of the macroscopic characteristics of the sample, which becomes milky and fluid. ε increase remains small, and yet corresponds to a very large increase of the bilayer area, to the point where R should theoretically diverge for a critical value of ε:

$$\varepsilon_{lim} = \frac{1}{q + 1}. \tag{4}$$

What is the physical meaning of R divergence? The physics underlying this transformation is related to the slight increase of lipids available for the bilayer but also to the progressive scarcity of DHPC available for the edges. If R is the radius of the disks, the area of the disks varies like R^2, whereas that of the edges varies like R. Above a critical value of ε, the increased DHPC partition into the bilayer section of the disks does not leave enough short-chain lipids to fill all the edges. Hence, bilayers have to fuse and give rise to lamellae of large size or reseal by forming vesicles, to reduce the edge volume. Large lamellae are more likely to bend than are small disks. Indeed, it is well known that sonicated vesicles have a minimum radius of ~100 Å, which corresponds to the maximum bending of a lipid bilayer.

Furthermore, if we refer to previous works on disk-to-vesicle transitions in presence of detergent, two important physical parameters are likely to take part in the structural transitions observed in DMPC/DHPC mixtures: the bending modulus of the bilayer and the line tension of edges (Lasic, 1982; Fromherz, 1983; Leng et al., 2003). The bending modulus depends on the bilayer composition (Bergström, 2001) and seems to decrease in the presence of detergent as shown in previous works (Otten et al., 1995; Brown et al., 2002). The fraction of DHPC in the bilayer increases when

the sample is heated, which may reduce the energetic cost of bending, facilitating undulation and, eventually, the spontaneous resealing to form a vesicle. Other physical parameters affecting the interactions between disks should also influence the transition to vesicles or to intermediate structures (Leng et al., 2003). At this stage, it seems difficult to predict T_v for different values of ε or q. Here again, of the existing models, only the mixed bicelle predicts the divergence of R, hence the sudden structural change.

Although ^{31}P-NMR may not be the ideal technique to explore certain situations (see the *dotted lines* in Fig. 8), our experiments show that there is no abrupt transition from bicelles to vesicles. The topological transition begins before the radius divergence and, for a certain temperature range, bicelles and vesicles coexist. To make a structural interpretation of the spectra obtained in this temperature domain, it is interesting to look at spectra obtained at 46°C for different q values (Fig. 4). As seen before, the values of the different critical temperatures (T_m, T_v, and T_h) depend on the sample composition and lowering q at a fixed temperature is equivalent to lowering the temperature at a fixed q. For each spectrum in Fig. 4 we will clarify below the corresponding temperature domain.
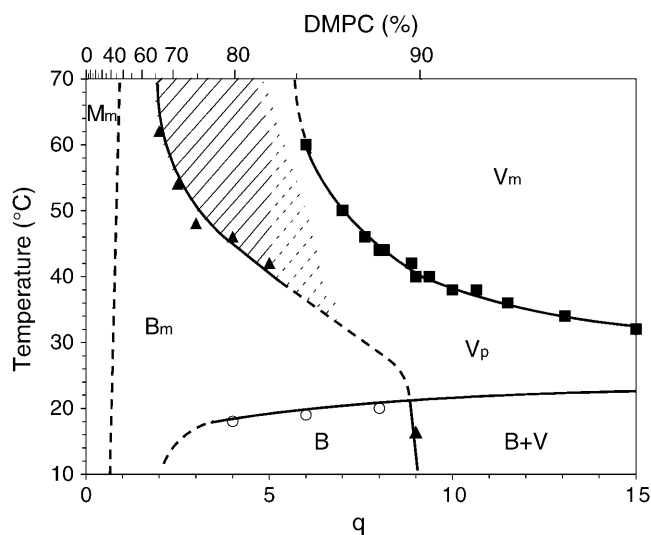

FIGURE 8 Tentative temperature/composition diagram of DMPC/DHPC mixtures, at a concentration in water of 25% (w/w), where we have emphasized the main conclusions of this article. This diagram is incomplete because we do not have the precise boundaries of all the domains that can be determined using our results (*dotted lines*). The limits determined with open circles, full triangles, and full squares correspond to T_m, T_v, and T_h, respectively. Below T_m, perfectly segregated bicelles (*B*) are found, coexisting with DMPC vesicles (*V*) at high q values. Above T_m, DHPC molecules enter the bilayer and start to form mixed bicelles (*Bm*). Above T_v, multilamellar vesicles form, starting with perforated vesicles (*Vp*), coexisting with remaining mixed bicelles (*shaded* zone). Finally, above T_h, bicelles and holes disappear because the vesicle bilayer is no longer saturated with DHPC, and only mixed vesicles (*Vm*) remain. For very low q values, mixed bicelles probably turn into mixed micelles (*Mm*).

$T \geq T_h$, lipid vesicles

At $T = T_h$, we have $\varepsilon = \varepsilon_{\text{lim}}$, which means that $[DHPC]_{\text{bilayer}} = [DHPC]$. Thus, for large q values and at high temperatures ($T \geq T_h$), only vesicles exist. This evolution is temperature dependent because the partition of short-chain lipids in the bilayer section is itself temperature dependent. In Fig. 4, the spectrum obtained for $q = 15$ and 46°C, i.e., for $T > T_h$ is, indeed, characteristic of vesicles. It is not surprising that for such ratio between the number of DMPC and DHPC molecules, the structure formed is close to that of a pure DMPC suspension. However, the line shape of the NMR spectrum indicates that vesicles are deformed by the magnetic field (Seelig et al., 1985; Pott and Dufourc, 1995; Picard et al., 1999). This kind of vesicle deformation in a magnetic field had already been observed by addition of detergent molecules $C_{12}E_8$ to DMPC bilayers (Otten et al., 1995). It was demonstrated that this phenomenon is provoked by a decrease in the bending modulus of the DMPC bilayer caused by the incorporation of the detergent (Otten et al., 2000). We believe that the DHPC incorporated in the vesicle also has a softening effect on the bilayer. This is confirmed by the fact that the signal around -15 ppm is more intense for $q = 10$ than for $q = 15$, indicating that when more DHPC is added the vesicles are more easily deformed.

$T_v \leq T \leq T_h$, perforated vesicles

If we keep looking at Fig. 4, when $q < 9$ the DHPC signal begins to differentiate from the signal of DMPC, indicating the existence of a new environment for DHPC. This is the case for example at $q = 7$ and $T = 46$°C. Because the shape of the DMPC signal at $q = 7$ is very close to that at $q = 10$, we propose that the new structures are perforated vesicles, also deformed by the magnetic field. The excess of DHPC forms holes in those vesicles. Simulated spectra obtained by considering ellipsoidal vesicles uniformly covered by DHPC holes confirmed this interpretation (Triba, 2003). This kind of structure has also been proposed from electron microscopy and small-angle neutron scattering for samples at high temperatures (Nieh et al., 2004; Van Dam et al., 2004).

In Fig. 4, we see that if q is lowered to $q = 6$, the signal of DHPC, which rapidly exchanges between edges and bilayers, shifts to lower fields. This indicates that a more important fraction of DHPC contributes to the holes. At $q = 4$, in addition to the signal assigned to perforated vesicles, two new ^{31}P resonances appear. Those lines are characteristic of the signals observed in the oriented domain ($2 < q < 6$ and $T_m < T < T_v$). Consequently, the spectrum obtained at $q = 4$ suggests that deformed perforated vesicles can coexist with aligned bicelles when $T_v \leq T < T_h$. When these two structures are present, we observe that signals of bicelles shift with increasing temperature toward lower fields, indicating that their radius diminishes. Eventually, the bicelle signals turn into a single isotropic signal. The resulting structure is

likely to be small mixed micelles or bicelles, coexisting with perforated vesicles (see Fig. 1 and *vertical arrows*).

Comparison with membrane solubilization by detergents

It is interesting to compare our general view of the interaction between DMPC and DHPC with results obtained by experiments designed to solubilize membranes with detergents (Ollivon et al., 1988, 2000; Edwards et al., 1989; Vinson et al., 1989; Chen and Szostak, 2004). DHPC can be considered as a mild detergent. When adding detergents to a vesicle suspension, they incorporate in the membrane until saturation. Adding more detergent often results in the formation of holes in the membranes (the excess detergent occupying the holes' edges) and new structures are formed by mixtures of detergents and lipids. Eventually, vesicles disappear and are replaced by micelles.

In our system, T_h is the temperature at which DHPC concentration reaches its saturation value in the DMPC bilayer. Above T_h, all DHPC molecules are in vesicle bilayers whereas below T_h holes are formed in the vesicles. Similarly, T_v is the temperature below which vesicles totally disappear. Between T_v and T_h, bicelles and perforated vesicles can coexist.

We are thus able to indirectly measure ε values independently from the method previously described because, at T_h:

$$\varepsilon = \varepsilon_{lim} = \frac{1}{q+1}. \qquad (5)$$

The full circles in Fig. 6 are deduced from this equation. The fact that both series of points are very close confirms that Gibbs' law is fulfilled, even above T_v. Indeed, as long as edges and bilayers coexist at a given temperature, ε represents the highest fraction of DHPC that can be accepted by the bilayers at this temperature.

SUMMARY AND CONCLUSION

A large amount of work on bicelle mixtures is based on the unrealistic hypothesis of a total segregation between the different lipids above T_m whereas experimental results only indicate that DMPC/DHPC miscibility is small. A total segregation above T_m is in disagreement with most experiments performed in the context of lipid mixtures phase diagrams and membrane solubilization studies (Lee, 1977; van Dijck et al., 1977; Ollivon et al., 1988, 2000; Edwards et al., 1989; Vinson et al., 1989; London and Brown, 2000; Chen and Szostak, 2004). This hypothesis also contradicts works on other lipidic discoidal structures and mixing entropy considerations (Mazer et al., 1980; Dubois et al., 2000).

If the partial miscibility of the two lipids had already been suggested before, we have measured for the first time the evolution with temperature of the DHPC miscibility in the bilayer. One of the most important results of our work is to show the important consequence of this miscibility, which has been overlooked in previous works: the rapid increase of

the proportion of bilayer area when the temperature is raised. The variation of the DHPC miscibility in the bilayer, although it remains small, is the driving force for the structural transitions observed when the sample is heated.

We have studied a great variety of samples and experimental conditions and we provide a model that is compatible with all observations. For example, in all cases, the ratio of the appropriate resonance areas is equal to q. Although DHPC miscibility is compatible with other orientable structures (perforated lamellae, wormlike micelles...), we have no reason to disprove the disk model below T_v. Above T_v, the perforated lamellae model is essentially a closeup on our perforated vesicles model (see Fig. 9). We have explained the transition between disks and perforated vesicles and we believe it reconciles both previously proposed structural models. In addition to suggesting structural models, we were very careful in checking that there were continuous transitions between these structural changes. Last but not least, we give an explanation for the driving force of these transitions.

Although we agree on the existence of perforated lamellae/vesicles at high temperatures, our model is still at conflict with the interpretations of authors who fit their data with perforated lamellae at intermediate temperatures, typically 35°C for $q = 3$ (Gaemers and Bax, 2001; Nieh et al., 2001, 2002; Soong and Macdonald, 2004). Because unperforated lamellae/vesicles exist at 55°C and perforated lamellae exist at 45°C, it is likely that the pore density increases when the temperature decreases. If perforated lamellae exist at intermediate temper-
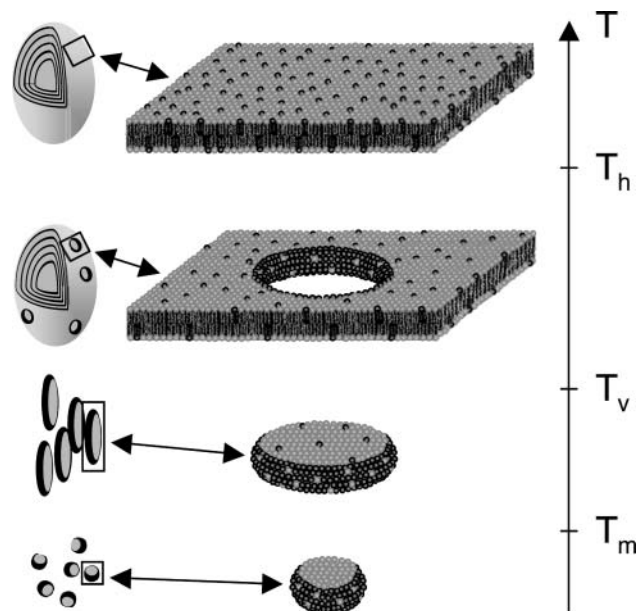

FIGURE 9 Cartoon of the various DMPC/DHPC structures encountered during this study, along with the main transition temperatures. From low to high temperatures are: small segregated bicelles (B); larger interacting mixed bicelles (Bm); large perforated multilamellar vesicles (Vp); large mixed multilamellar vesicles (Vm). Light lipids represent DMPC whereas dark lipids represent DHPC. The structures are represented at different scales.

atures, they may be highly perforated and fragile enough to be transiently broken by thermal fluctuations. In that case, it becomes merely a semantic issue to decide to call these objects perforated lamellae rather than ''disks making transient contacts on an edge-on manner'', an hypothesis also considered by Gaemers and Bax (2001) to fit their own NMR diffusion data.

To summarize the results of this investigation we have drawn a tentative temperature/composition diagram of DMPC/DHPC mixtures, at a concentration in water of 25% (w/w), where we have emphasized the main conclusions (Fig. 8). This diagram is incomplete because we do not have the precise boundaries of all the domains that can be defined. Furthermore, had we allowed the lipid concentration to vary, it is likely that the other parameters would have been changed and a complete structural diagram would have required a three-dimensional figure. Researchers working on bicelles have mostly studied the domain where DHPC molecules are >15% of the total lipids ($q \leq 6$). In this domain, we have determined four meaningful temperature ranges: below T_m; between T_m and T_v; between T_v and T_h; above T_h. All boundaries were determined here through observation of ^{31}P-NMR spectra even though other techniques could be used and may be more accurate in specific cases.

T_h is the temperature for which holes disappear from vesicle surfaces when the temperature is increased. Above T_h, DHPC penetrates the mixed vesicles (Vm) without perforating them. There is no reason, a priori, for these vesicles to be unilamellar. Just below T_h, perforated vesicles appear (Vp), but the proportion of DHPC available is too small to ''solubilize'' the membranes. Only holes can be formed by DHPC. Simultaneously, or at a slightly lower temperature, mixed bicelles (Bm) can appear and coexist with the perforated vesicles. This coexistence domain is represented by a shadow in the diagram. Below T_v the perforated vesicles disappear and only bicelles are present in the sample. In the usually investigated region ($T_m < T < T_v$ and $q \leq 6$), we have shown that bicelles alignment improved when their radius was increased with temperature. At $T \approx T_m$, a broad signal appears, which is an indication that bicelles are not well oriented and that disk tumbling is slow. Below T_m, lipids form small, rapidly tumbling, almost perfectly segregated disks (B). If DMPC is in excess ($q > 8$), these disks coexist with pure DMPC vesicles in the gel phase (V). If q is very low, mixed micelles (Mm) are likely to replace the bicelles. A cartoon of the various structures encountered in this study is drawn in Fig. 9.

Using mostly ^{31}P-NMR, our understanding of the DMPC/DHPC diagram is now greatly improved. Some extreme conditions (q close to zero for example) and some boundaries could be determined more accurately using other techniques (calorimetry for example). Nevertheless, we have to keep in mind that our main objective is to understand and to use bicelles as a good membrane mimic, and to control their alignment in the magnetic field. For that matter, the diagram we have determined is very useful, as we know that the best bicellar alignment is just below T_v. We also know that T_v can be adjusted to be physiologically relevant by choosing an appropriate q value. As an example, if one wants to use bicelles at 37°C, the ideal q value is 5 rather than 3, which is commonly used. Transition temperatures can be further adjusted by customizing the nature of the lipids used. This will be the subject of a later article.

APPENDIX 1: THEORETICAL CONSIDERATIONS ON ^{31}P-NMR SPECTRA OF BICELLE LIPID MIXTURES ABOVE T_M

In this appendix we establish a relation between DHPC and DMPC ^{31}P chemical shifts, ω_{DHPC} and ω_{DMPC}, respectively.

The quantity $\Delta\omega_{DHPC}/\Delta\omega_{DMPC} = (\omega_{DHPC} - \omega_{DHPC}^{iso})/(\omega_{DMPC} - \omega_{DMPC}^{iso})$ will be expressed as a function of q and ε.

As shown experimentally, the isotropic frequencies of DHPC and DMPC are slightly different ($\omega_{DMPC}^{iso} - \omega_{DHPC}^{iso} \approx 0.1$ ppm). Considering the splitting between DMPC and DHPC (>4 ppm), this difference is negligible in the oriented temperature domain. Thus, we make the approximation $\omega_{DMPC}^{iso} \approx \omega_{DHPC}^{iso} \approx \omega^{iso}$.

To obtain the ^{31}P resonance frequencies of phospholipids in bicelles or in perforated lamellae, the motions of the phospholipids headgroups are decomposed into several motions with axial symmetry that remain independent from one another (Zandomeneghi et al., 2003). For a lipid l, we obtain:

$$\omega_l = \omega^{iso} + \frac{1}{2}(3\cos^2\theta - 1)\overline{\delta}_l \times S_{bilayer}, \qquad (A1)$$

where θ is the angle between the magnetic field $\mathbf{B_0}$ and the average orientation of the bilayer, $S_{bilayer}$ is the order parameter describing the motions of the bilayer normal with respect to its average orientation and $\overline{\delta}_l$ is the average chemical shift anisotropy in the bilayer frame (Zandomeneghi et al., 2003). $\overline{\delta}_l$ is a function of lipid headgroup motions with respect to the bilayer that can, a priori, be different for DHPC and DMPC although both lipids bear the same phosphatidylcholine headgroup.

In a strong magnetic field, most bicelles have their average bilayer normal perpendicular to $\mathbf{B_0}$ (i.e., $\theta = 90°$). Because of the mosaic spread, resonances are slightly asymmetric but their maximum ^{31}P frequency (the 90° edge) is:

$$\omega_l = \omega^{iso} - \frac{1}{2}\overline{\delta}_l \times S_{bilayer}. \qquad (A2)$$

If bicelles were static, $S_{bilayer}$ would be equal to 1. But they oscillate rapidly (on a ^{31}P-NMR timescale) in a cone around their average orientation. The Gaussian aperture of this cone, characterized by Σ, can be estimated by measuring the ^{31}P chemical shift ω_{DMPC} of DMPC, knowing that (Schmidt-Rohr and Spiess, 1994):

$$S_{bilayer} = \frac{\int_0^{90°} e^{-\frac{\sin^2\theta}{2\Sigma^2}} \times \frac{1}{2}(3\cos^2\theta - 1) \times \sin\theta \times d\theta}{\int_0^{90°} e^{-\frac{\sin^2\theta}{2\Sigma^2}} \times \sin\theta \times d\theta}.$$

For $q > 2$, one can neglect the amount of DMPC in the edges, we are left with $\overline{\delta}_{DMPC}$, $\overline{\delta}_{DHPC}^{bilayer}$, and $\overline{\delta}_{DHPC}^{edge}$. In addition, if we make the hypothesis that DHPC exchanges rapidly between bilayer and edges, the frequency of the DHPC signal can be given by:

$$\omega_{DHPC} = \frac{n_{DHPC}^{edge}}{n_{DHPC}} \times \omega_{DHPC}^{edge} + \frac{n_{DHPC}^{bilayer}}{n_{DHPC}} \times \omega_{DHPC}^{bilayer},$$

where n_{DHPC}, $n_{\text{DHPC}}^{\text{edge}}$, and $n_{\text{DHPC}}^{\text{bilayer}}$ are, respectively, the total number of DHPC molecules, the number of DHPC molecules in the edges and the number of DHPC molecules in the bilayer. Using the definition of ε and q we obtain:

$$\omega_{\text{DHPC}} = \left(1 - \frac{\varepsilon}{1-\varepsilon} \times q\right) \times \omega_{\text{DHPC}}^{\text{edge}} + \left(\frac{\varepsilon}{1-\varepsilon} \times q\right) \times \omega_{\text{DHPC}}^{\text{bilayer}}. \tag{A3}$$

We have carried out experiments at $T > T_{\text{m}}$ with large q values, up to $q = 15$. In such a case, only one signal is observed in the ^{31}P-NMR spectra for temperatures at which orientation is classically observed (30–45°C). This confirms that, for such temperatures, DHPC has a very high partition coefficient in favor of the lipid bilayer and that DHPC polar head, once in a lipid bilayer, experiences the same dynamics as DMPC polar head. These experiments also confirm that the dynamics of the DMPC polar head is unaffected by the presence of DHPC in the bilayer. This makes ^{31}P-NMR a favorable case for studying bicelles as we can make another simplification, namely $\bar{\delta}_{\text{DHPC}}^{\text{bilayer}} \approx \bar{\delta}_{\text{DMPC}} \approx 30\,\text{ppm}$. This simplification would also be justified if looking at carbonyl ^{13}C resonances but not if the spins observed were located in the lipid chains, as pointed out by Sanders and Schwonek for some ^{2}H-NMR experiments (Sanders and Schwonek, 1992).

Finally, Eqs. A2 and A3 can be rewritten as follows:

$$\frac{\Delta\omega_{\text{DHPC}}}{\Delta\omega_{\text{DMPC}}} = \left(1 - \frac{\bar{\delta}_{\text{DHPC}}^{\text{edge}}}{\bar{\delta}_{\text{DMPC}}}\right) \times \frac{\varepsilon}{1-\varepsilon} \times q + \frac{\bar{\delta}_{\text{DHPC}}^{\text{edge}}}{\bar{\delta}_{\text{DMPC}}}. \tag{A4}$$

This formula is similar to the formula 6 in the article by Sanders and Schwonek (1992) although in our case we do not assume, as they did implicitly, the same local dynamics for lipids on the bilayer surface and in the edges.

APPENDIX 2: GEOMETRICAL IMPLICATIONS OF THE MIXED BICELLE MODEL

Expressions of the bicelle radius, which were proposed until now, were obtained by considering the ratio between the surface occupied by the bilayer and the surface occupied by the edge (Vold and Prosser, 1996). As explained in the text, we believe that a more appropriate method is to consider the ratio between volumes instead of surfaces. Another improvement was made by using an edge with an elliptical cross section as shown in Fig. 7 b.

If q_{v} is the ratio of the volume occupied by the bilayer, V_{bilayer}, divided by the volume occupied by the edges, V_{edge}, then:

$$q_{\text{v}} = \frac{V_{\text{bilayer}}}{V_{\text{edge}}}. \tag{A5}$$

The volume of the elliptical edge is given by:

$$V_{\text{edge}} = \pi r_{\perp} r_{//} \times \left(\pi R + \frac{4}{3} r_{\perp}\right), \tag{A6}$$

whereas the volume of the disk bilayer is given by:

$$V_{\text{bilayer}} = 2r_{//} \times \pi R^2. \tag{A7}$$

Incorporating Eqs. A6 and A7 into Eq. A5 we find:

$$R = \frac{1}{4} r_{\perp} q_{\text{v}} \left(\pi + \sqrt{\pi^2 + \frac{32}{3q_{\text{v}}}}\right). \tag{A8}$$

Let us write $n_{\text{DMPC}}^{\text{bilayer}}$ and $n_{\text{DMPC}}^{\text{edge}}$ the number of DMPC molecules, respectively, in the bilayer and in the edge, and $n_{\text{DHPC}}^{\text{bilayer}}$ and $n_{\text{DHPC}}^{\text{edge}}$ the number of DHPC molecules, respectively, in the bilayer and in the edge. If v_{DHPC} and v_{DMPC} are, respectively, the volume of a molecule of DHPC and that of DMPC, we have:

$$q_{\text{v}} = \frac{n_{\text{DMPC}}^{\text{bilayer}} \times v_{\text{DMPC}} + n_{\text{DHPC}}^{\text{bilayer}} \times v_{\text{DHPC}}}{n_{\text{DMPC}}^{\text{edge}} \times v_{\text{DMPC}} + n_{\text{DHPC}}^{\text{edge}} \times v_{\text{DHPC}}}.$$

If λ is the ratio between v_{DHPC} and v_{DMPC}, using the definition of q, ε, and ε' we find that:

$$q_{\text{v}} = \frac{q - \varepsilon'(q+1)}{\lambda + \varepsilon'(1-\lambda)} \times \left[\frac{1 + \varepsilon(\lambda-1)}{1 - \varepsilon(q+1)}\right]. \tag{A9}$$

For $q > 2$ and $\varepsilon' \ll 1$, the number of DMPC molecules located in the edges can be neglected ($n_{\text{DMPC}}^{\text{edge}} \ll n_{\text{DMPC}}^{\text{bilayer}}$) and we can write $n_{\text{DMPC}}^{\text{bilayer}} \approx n_{\text{DMPC}}$

$$q_{\text{v}} \approx \frac{n_{\text{DMPC}} \times v_{\text{DMPC}} + n_{\text{DHPC}}^{\text{bilayer}} \times v_{\text{DHPC}}}{n_{\text{DHPC}}^{\text{edge}} \times v_{\text{DHPC}}}$$

$$q_{\text{v}} \approx \frac{q}{\lambda} \times \left[\frac{1 + \varepsilon(\lambda-1)}{1 - \varepsilon(q+1)}\right]. \tag{A10}$$

Incorporating Eq. A10 into Eq. A8 allows us to draw the curves shown in Fig. 7, c and d. The simplified formula of R is given by:

$$R \approx \frac{\pi}{2} r_{\perp} \times \frac{q}{\lambda} \times \left[\frac{1 + \varepsilon(\lambda-1)}{1 - \varepsilon(q+1)}\right]. \tag{A11}$$

REFERENCES

Arnold, A., T. Labrot, R. Oda, and E. J. Dufourc. 2002. Cation modulation of bicelle size and magnetic alignment as revealed by solid-state NMR and electron microscopy. *Biophys. J.* 83:2667–2680.

Bergström, M. 2001. Molecular interpretation of the mean bending constant for a thermodynamically open vesicle bilayer. *Langmuir.* 17:7675–7686.

Bian, J. R., and M. F. Roberts. 1990. Phase separation in short-chain lecithin/gel-state long-chain lecithin aggregates. *Biochemistry.* 29:7928–7935.

Bolze, J., T. Fujisawa, T. Nagao, K. Norisada, H. Saitô, and A. Naito. 2000. Small angle X-ray scattering and 31P NMR studies on the phase behavior of phospholipid bilayered mixed micelles. *Chem. Phys. Lett.* 329:215–220.

Brown, M. F., R. L. Thurmond, S. W. Dodd, D. Otten, and K. Beyer. 2002. Elastic deformation of membrane bilayers probed by deuterium NMR relaxation. *J. Am. Chem. Soc.* 124:8471–8484.

Cevc, G., and D. Marsh. 1987. Phospholipid Bilayers: Physical Principles and Models. John Wiley and Sons, New York, NY.

Chen, I. A., and J. W. Szostak. 2004. A kinetic study of the growth of fatty acid vesicles. *Biophys. J.* 87:988–998.

Dubois, M., L. Belloni, T. Zemb, B. Demé, and T. Gulik-Krzywicki. 2000. Formation of rigid nanodiscs: edge formation and molecular separation. *Prog. Colloid Polym.* 115:238–242.

Duneau, J.-P., A.-H. Saifi, and J. Sturgis. 2003. DHPC-DMPC-water phase diagram at high water content. *Eur. Biophys. J.* 32:289.

Edwards, K., M. Almgren, J. Bellare, and W. Brown. 1989. Effects of Triton X-100 on sonicated lecithin vesicles. *Langmuir.* 147:473–478.

Eum, K. M., G. Riedy, K. H. Langley, and M. F. Roberts. 1989. Temperature-induced fusion of small unilamellar vesicles formed from saturated long-chain lecithins and diheptanoylphosphatidylcholine. *Biochemistry.* 28:8206–8213.

Feigenson, G. W., and J. T. Buboltz. 2001. Ternary phase diagram of dipalmitoyl-PC/dilauroyl-PC/cholesterol: nanoscopic domain formation driven by cholesterol. *Biophys. J.* 80:2775–2788.

Fromherz, P. 1983. Lipid-vesicle structure: size control by edge-active agents. *Chem. Phys. Lett.* 94:259–266.

Gabriel, N. E., N. V. Agman, and M. F. Roberts. 1987. Enzymatic hydrolysis of short-chain lecithin/long-chain phospholipid unilamellar vesicles: sensitivity of phospholipases to matrix phase state. *Biochemistry.* 26:7409–7418.

Gabriel, N. E., and M. F. Roberts. 1984. Spontaneous formation of stable unilamellar vesicles. *Biochemistry.* 23:4011–4015.

Gabriel, N. E., and M. F. Roberts. 1986. Interaction of short-chain lecithin with long-chain phospholipids: characterization of vesicles that form spontaneously. *Biochemistry.* 25:2812–2821.

Gabriel, N. E., and M. F. Roberts. 1987. Short-chain lecithin/long-chain phospholipid unilamellar vesicles: asymmetry, dynamics, and enzymatic hydrolysis of the short-chain component. *Biochemistry.* 26:2432–2440.

Gaemers, S., and A. Bax. 2001. Morphology of three lyotropic liquid crystalline biological NMR media studied by translational diffusion anisotropy. *J. Am. Chem. Soc.* 123:12343–12352.

Glover, K. J., J. A. Whiles, R. R. Vold, and G. Melacini. 2002. Position of residues in transmembrane peptides with respect to the lipid bilayer: a combined lipid Noes and water chemical exchange approach in phospholipid bicelles. *J. Biomol. NMR.* 22:57–64.

Glover, K. J., J. A. Whiles, M. J. Wood, G. Melacini, E. A. Komives, and R. R. Vold. 2001a. Conformational dimorphism and transmembrane orientation of prion protein residues 110–136 in bicelles. *Biochemistry.* 40:13137–13142.

Glover, K. J., J. A. Whiles, G. Wu, N. Yu, R. Deems, J. O. Struppe, R. E. Stark, E. A. Komives, and R. R. Vold. 2001b. Structural evaluation of phospholipid bicelles for solution-state studies of membrane-associated biomolecules. *Biophys. J.* 81:2163–2171.

Hare, B. J., J. H. Prestegard, and D. M. Engelman. 1995. Small angle x-ray scattering studies of magnetically oriented lipid bilayers. *Biophys. J.* 69:1891–1896.

Howard, K. P., and S. J. Opella. 1996. High-resolution solid-state NMR spectra of integral membrane proteins reconstituted into magnetically oriented phospholipid bilayers. *J. Magn. Reson. B.* 112:91–94.

Lasic, D. D. 1982. A molecular model for vesicle formation. *Biochim. Biophys. Acta.* 692:501–502.

Lee, A. G. 1977. Lipid phase transitions and phase diagrams. II. Mixtures involving lipids. *Biochim. Biophys. Acta.* 472:285–344.

Leng, J., S. U. Egelhaaf, and M. E. Cates. 2003. Kinetics of the micelle-to-vesicle transition: aqueous lecithin-bile salt mixtures. *Biophys. J.* 85:1624–1646.

Lin, T.-L., C.-C. Liu, M. F. Roberts, and S.-H. Chen. 1991. Structure of mixed short-chain lecithin/long-chain lecithin aggregates studied by small-angle neutron scattering. *J. Phys. Chem.* 95:6020–6027.

Lindberg, M., H. Biverstahl, A. Graslund, and L. Maler. 2003. Structure and positioning comparison of two variants of penetratin in two different membrane mimicking systems by NMR. *Eur. J. Biochem.* 270:3055–3063.

London, E., and D. A. Brown. 2000. Insolubility of lipids in triton X-100: physical origin and relationship to sphingolipid/cholesterol membrane domains (rafts). *Biochim. Biophys. Acta.* 1508:182–195.

Luchette, P. A., T. N. Vetman, R. S. Prosser, R. E. Hancock, M. P. Nieh, C. J. Glinka, S. Krueger, and J. Katsaras. 2001. Morphology of fast-tumbling bicelles: a small angle neutron scattering and NMR study. *Biochim. Biophys. Acta.* 1513:83–94.

Mazer, N. A., G. B. Benedek, and M. C. Carey. 1980. Quasielastic light-scattering studies of aqueous biliary lipid systems. Mixed micelle formation in bile salt-lecithin solutions. *Biochemistry.* 19:601–615.

Nieh, M. P., C. J. Glinka, S. Krueger, R. S. Prosser, and J. Katsaras. 2001. SANS study on the structural phases of magnetically alignable lanthanide-doped phospholipid mixtures. *Langmuir.* 17:2629–2638.

Nieh, M. P., C. J. Glinka, S. Krueger, R. S. Prosser, and J. Katsaras. 2002. SANS study on the effect of lanthanide ions and charged lipids on the morphology of phospholipid mixtures. *Biophys. J.* 82:2487–2498.

Nieh, M. P., V. A. Raghunathan, C. J. Glinka, T. A. Harroun, G. Pabst, and J. Katsaras. 2004. Magnetically alignable phase of phospholipid ''bicelle'' mixtures is a chiral nematic made up of wormlike micelles. *Langmuir.* 20:7893–7897.

Ollivon, M., O. Eidelman, R. Blumenthal, and A. Walter. 1988. Micelle-vesicle transition of egg phosphatidylcholine and octyl glucoside. *Biochemistry.* 27:1695–1703.

Ollivon, M., S. Lesieur, C. Grabielle-Madelmont, and M. Paternostre. 2000. Vesicle reconstitution from lipid-detergent mixed micelles. *Biochim. Biophys. Acta.* 1508:34–50.

Otten, D., M. F. Brown, and K. Beyer. 2000. Softening of membrane bilayers by detergents elucidated by deuterium NMR spectroscopy. *J. Phys. Chem. B.* 104:12119–12129.

Otten, D., L. Lobbecke, and K. Beyer. 1995. Stages of the bilayer-micelle transition in the system phosphatidylcholine-C12E8 as studied by deuterium- and phosphorous-NMR, light scattering, and calorimetry. *Biophys. J.* 68:584–597.

Ottiger, M., and A. Bax. 1998. Characterization of magnetically oriented phospholipid micelles for measurement of dipolar couplings in macromolecules. *J. Biomol. NMR.* 12:361–372.

Picard, F., M. J. Paquet, J. Levesque, A. Belanger, and M. Auger. 1999. 31P NMR first spectral moment study of the partial magnetic orientation of phospholipid membranes. *Biophys. J.* 77:888–902.

Pott, T., and E. J. Dufourc. 1995. Action of melittin on the DPPC-cholesterol liquid-ordered phase: a solid state 2H-and 31P-NMR study. *Biophys. J.* 68:965–977.

Prosser, R. S., H. Bryant, R. G. Bryant, and R. R. Vold. 1999. Lanthanide chelates as bilayer alignment tools in NMR studies of membrane-associated peptides. *J. Magn. Reson.* 141:256–260.

Raffard, G., S. Steinbruckner, A. Arnold, J. H. Davis, and E. J. Dufourc. 2000. Temperature-composition diagram of dimyristoylphosphatidylcholine dicaproylphosphatidylcholine ''bicelles'' self-orienting in the magnetic field. A solid state 2H and 31P NMR study. *Langmuir.* 16:7655–7662.

Ramirez, B. E., O. N. Voloshin, R. D. Camerini-Otero, and A. Bax. 2000. Solution structure of DinI provides insight into its mode of RecA inactivation. *Protein Sci.* 9:2161–2169.

Rowe, B. A., and S. L. Neal. 2003. Fluorescence probe study of bicelle structure as a function of temperature: developing a practical bicelle structure model. *Langmuir.* 19:2039–2048.

Sanders, C. R., 2nd, and G. C. Landis. 1994. Facile acquisition and assignment of oriented sample NMR spectra for bilayer surface-associated proteins. *J. Am. Chem. Soc.* 116:6470–6471.

Sanders, C. R., 2nd, and G. C. Landis. 1995. Reconstitution of membrane proteins into lipid-rich bilayered mixed micelles for NMR studies. *Biochemistry.* 34:4030–4040.

Sanders, C. R., 2nd, and J. P. Schwonek. 1992. Characterization of magnetically orientable bilayers in mixtures of dihexanoylphosphatidylcholine and dimyristoylphosphatidylcholine by solid-state NMR. *Biochemistry.* 31:8898–8905.

Schmidt-Rohr, K., and H. W. Spiess. 1994. Multidimensional solid-state NMR and polymers. Academic Press, London, UK.

Seelig, J., F. Borle, and T. A. Cross. 1985. Magnetic ordering of phospholipid membranes. *Biochim. Biophys. Acta.* 814:195–198.

Small, D. M. 1986. The Physical Chemistry of Lipids: From Alkanes to Phospholipids. Plenum Press, New York, NY.

Soong, R., and P. M. Macdonald. 2004. Lateral diffusion of PEG-lipid in magnetically aligned bicelles measured using stimulated echo pulsed field gradient 1H NMR. *Biophys. J.* 88:255–68.

Spalla, O. 2000. Long-range attraction between surfaces: existence and amplitude? *Curr. Opin. Colloid Interface Sci.* 5:5–12.

Sternin, E., D. Nizza, and K. Gawrisch. 2001. Temperature dependence of DMPC/DHPC mixing in a bicellar solution and its structural implications. *Langmuir*. 17:2610–2616.

Struppe, J., and R. R. Vold. 1998. Dilute bicellar solutions for structural NMR work. *J. Magn. Reson*. 135:541–546.

Tanford, C. 1991. The hydrophobic effect: formation of micelles and biological membranes, 2nd ed. John Wiley and Sons. New York, NY.

Tjandra, N., and A. Bax. 1997. Direct measurement of distances and angles in biomolecules by NMR in a dilute liquid crystalline medium. *Science*. 278:1111–1114.

Triba, M. N. 2003. Etude physico-chimique de bicelles par RMN du phosphore-31. PhD thesis. Université Denis Diderot, Paris.

Van Dam, L., G. Karlsson, and K. Edwards. 2004. Direct observation and characterization of DMPC/DHPC aggregates under conditions relevant for biological solution NMR. *Biochim. Biophys. Acta*. 1664:241–256.

van der Kooij, F. M., K. Kassapidou, and H. N. W. Lekkerkerker. 2000. Liquid crystal phase transitions in suspensions of polydisperse plate-like particles. *Nature*. 406:868–871.

van Dijck, P. W., A. J. Kaper, H. A. Oonk, and J. de Gier. 1977. Miscibility properties of binary phosphatidylcholine mixtures. A calorimetric study. *Biochim. Biophys. Acta*. 470:58–69.

Vinson, P. K., Y. Talmon, and A. Walter. 1989. Vesicle-micelle transition of phosphatidylcholine and octyl glucoside elucidated by cryo-transmission electron microscopy. *Biophys. J*. 56:669–681.

Vold, R. R., and R. S. Prosser. 1996. Magnetically oriented phospholipid bilayered micelles for structural studies of polypeptides. Does the ideal bicelle exist? *J. Magn. Reson. B*. 113:267–271.

Vold, R. R., R. S. Prosser, and A. J. Deese. 1997. Isotropic solutions of phospholipid bicelles: a new membrane mimetic for high-resolution NMR studies of polypeptides. *J. Biomol. NMR*. 9:329–335.

Zandomeneghi, G., M. Tomaselli, P. T. Williamson, and B. H. Meier. 2003. NMR of bicelles: orientation and mosaic spread of the liquid-crystal director under sample rotation. *J. Biomol. NMR*. 25:113–123.